Inorganic Chemistry
Cite This: *Inorg. Chem.* XXXX, XXX, XXX−XXX
Forum Article
pubs.acs.org/IC

When Do Strongly Coupled Diradicals Show Strongly Coupled Reactivity? Thermodynamics and Kinetics of Hydrogen Atom Transfer Reactions of Palladium and Platinum Bis(iminosemiquinone) Complexes

Kyle M. Conner, AnnaMaria C. Arostegui, Daniel D. Swanson, and Seth N. Brown*

Department of Chemistry and Biochemistry, University of Notre Dame, 251 Nieuwland Science Hall, Notre Dame, Indiana 46556-5670, United States

Supporting Information

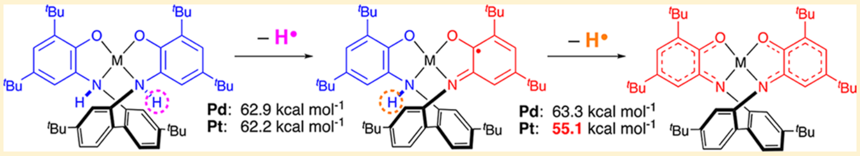

ABSTRACT: The 2,2′-biphenylene-bridged bis(iminosemiquinone) complexes (^{t}BuClip)M [^{t}BuClipH$_4$ = 4,4′-di-*tert*-butyl-*N*,*N*′-bis(3,5-di-*tert*-butyl-2-hydroxyphenyl)-2,2′-diaminobiphenyl; M = Pd, Pt] can be reduced to the bis(aminophenoxide) complexes (^{t}BuClipH$_2$)M by reaction with hydrazobenzene (M = Pd) or by catalytic hydrogenation (M = Pt). The palladium complex with one aminophenoxide ligand and one iminosemiquinone ligand, (^{t}BuClipH)Pd, is generated by comproportionation of (^{t}BuClip)Pd with (^{t}BuClipH$_2$)Pd in a process that is both slow (0.06 M^{-1} s^{-1} in toluene at 23 °C) and only modestly favorable (K_{com} = 1.9 in CDCl$_3$), indicating that both N−H bonds have essentially the same bond strength. The mono(iminoquinone) complex (^{t}BuClipH)Pt has not been observed, indicating that the platinum analogue shows no tendency to comproportionate (K_{com} < 0.1). The average bond dissociation free energies (BDFE) of the complexes have been established by equilibration with suitably substituted hydrazobenzenes, and the palladium bis(iminosemiquinone) is markedly more oxidizing than the platinum compound, with hydrogen transfer from (^{t}BuClipH$_2$)Pt to (^{t}BuClip)Pd occurring with $\Delta G°$ = −8.9 kcal mol^{-1}. The palladium complex (^{t}BuClipH$_2$)Pd reacts with nitroxyl radicals in two observable steps, with the first hydrogen transfer taking place slightly faster than the second. In the platinum analogue, the first hydrogen transfer is much slower than the second, presumably because the N−H bond in the monoradical complex (^{t}BuClipH)Pt is unusually weak. Using driving force−rate correlations, it is estimated that this bond has a BDFE of 55.1 kcal mol^{-1}, which is 7.1 kcal mol^{-1} weaker than that of the first N−H bond in (^{t}BuClipH$_2$)Pt. The two radical centers in the platinum, but not the palladium, complex thus act in concert with each other and display a strong thermodynamic bias toward two-electron reactivity. The greater thermodynamic and kinetic coupling in the platinum complex is attributed to the stronger metal−ligand π interactions in this compound.

INTRODUCTION

The term “radical” is freighted with a connotation of “reactive”; it is ingrained in chemists that free radicals are highly reactive. Yet a moment’s reflection by any inorganic chemist will indicate the peculiarity of this reflex: the defining feature of a radical, the presence of an unpaired electron, is not in and of itself associated with any particular reactivity. Transition-metal complexes with one or more unpaired electrons are common and are not possessed of special reactivity. Indeed, Hund’s rule indicates that species with greater numbers of unpaired electrons should, all other things being equal, be more stable than those with fewer unpaired electrons. This expectation is borne out chemically, for example, in the notably higher thermodynamic and kinetic reactivity of singlet dioxygen compared to triplet dioxygen.

Of course, many free radicals are highly reactive, but this is not principally due to unpaired electrons per se but rather the common association of the presence of an unpaired electron with the opportunity for the molecule to engage in one-electron chemistry of various sorts—dimerization, atom abstraction, addition to unsaturated molecules, etc.—in order to increase its bonding. Many radicals can easily form additional strong bonds, and it is this high driving force that creates reactivity.[1] When steric or electronic effects combine to decrease the propensity of radicals to form additional bonds, then persistent or isolable radicals of modest reactivity result.[2] Familiar examples from organic chemistry include nitroxyl radicals. Of more relevance to this Forum, transition metals are well-known to be able to stabilize radicals. A classic example of this stabilization is found with semiquinone radicals. These can exhibit some stability as free organic radicals, but they form highly stable inorganic

Special Issue: Applications of Metal Complexes with Ligand-Centered Radicals

Received: January 8, 2018

DOI: 10.1021/acs.inorgchem.8b00068
Inorg. Chem. XXXX, XXX, XXX−XXX

complexes where the metal center can dramatically tune their electronic properties and give rise to species of controlled reactivity.[3] This moderation of the reactivity is of considerable interest in the development of reactive species based on coordinated radicals[4] because efficient catalysis requires reagents that operate with low kinetic barriers at only modest thermodynamic driving forces.

One intrinsic problem, however, in realizing this efficient reactivity is the disconnect between the one-electron reactivity of radicals and the thermodynamic predilection of organic substrates to undergo two-electron reactions. For example, gas-phase dehydrogenation of ethane to form ethylene (and H_2) is endothermic by a modest 32.6 kcal mol^{-1}, but formation of the ethyl radical (and 0.5 H_2) requires 48.5 kcal mol^{-1}.[5] If one is restricted to one-electron reactions such as hydrogen atom abstraction, one builds in an intrinsic thermodynamic barrier (an overpotential, in electrochemical terms) that necessarily implies a waste of energy. Any oxidant capable of oxidizing ethane to an ethyl radical is grossly overpowered (by 64 kcal mol^{-1}!) for oxidizing an ethyl radical to ethylene. Insofar as organic radicals with β-hydrogen atoms are unstable with respect to disproportionation, this analysis is general for other examples of dehydrogenation (such as alcohols to aldehydes or ketones). Other two-electron oxidations, such as hydroxylation, also suffer this thermodynamic bias; for example, oxidation of ethane to an ethyl radical by a hydroxyl radical is 75 kcal mol^{-1} more endothermic than the subsequent oxidation of an ethyl radical to ethanol.[5] Even in enzymes that operate by a rebound mechanism, where the oxidant that reacts with the initially formed radical need not be as powerful as the one that abstracts the initial hydrogen atom, this overpotential appears to be common. For example, calculations on the cytochrome P450 oxidation of methane estimate that the rebound step is about 65 kcal mol^{-1} more exothermic than the initial hydrogen atom abstraction.[6] This exothermicity cannot appreciably assist the kinetics of the reaction, which are dominated by the barrier to the initial hydrogen atom abstraction. Of course, many reactions of hydrocarbons do take place by radical mechanisms, but they must have a significant driving force if they are to occur at reasonable rates. Reactions with low driving forces, such as acceptorless dehydrogenation of alkanes, do not involve one-electron intermediates if they occur at reasonable rates at moderate temperatures.[7]

If one-electron oxidants such as metal-bound radicals are to react efficiently with organic substrates, they must have some way of coordinating their action so that two one-electron centers can act simultaneously on a substrate. One way to favor such concerted two-electron reactivity is for the reactivity of the two one-electron centers to be strongly coupled; in other words, engagement of the first redox center in one-electron reactions (such as hydrogen atom transfer) should strongly increase the propensity of the second redox center to do so as well. This kind of linkage between two one-electron events finds a parallel in hydrogen atom transfer chemistry, where the strong interdependence between proton- and electron-transfer events in a chemical system creates a strong thermodynamic bias for concerted, proton-coupled electron transfer over stepwise pathways.[8]

In fact, when multiple organic radicals are coordinated to a single transition-metal center, very strong communication between the radicals is the rule rather than the exception. A canonical example of this phenomenon is given by bis(iminosemiquinone) complexes of palladium(II) and platinum(II).[9−14] The electronic structures of these compounds are well described as "singlet diradicals": the compounds are diamagnetic but have open-shell character with substantial configuration interaction.[15] We recently undertook a study to measure the singlet−triplet gaps in these compounds and found gaps of ∼1800 cm^{-1} for the palladium compounds and ∼3000 cm^{-1} for the platinum compounds. In both cases, the radicals are thus very strongly coupled, with the larger coupling in the platinum compounds is due to stronger metal−ligand (anti)bonding interactions.[16]

Given such strong interradical communication, these bis(iminosemiquinone) complexes would seem to be ideal candidates to test whether diradical complexes can achieve the kind of kinetic or thermodynamic coupling in chemical reactions that could lead to efficient multielectron transformations. To date, the only chemistry reported for these complexes is outer-sphere redox chemistry, where one- and two-electron-oxidized or -reduced compounds can be generated and, in many cases, isolated.[13] In contrast, monoligated complexes appear to be somewhat more reactive; for example, a bimetallic (cyclooctadiene)platinum complex of a bis(amidophenoxide) has been shown to deliver electrons from the amidophenoxide and protons from the bound olefin to reduce an *o*-quinone.[17] Here we prepare the chelating bis(aminophenoxide) complexes of palladium(II) and platinum(II) based on the tetradentate 4,4′-di-*tert*-butyl-*N*,*N*′-bis(3,5-di-*tert*-butyl-2-hydroxyphenyl)-2,2′-diaminobiphenyl (^{t}BuClipH_4)[18] ligand. The bis(aminophenoxide) complexes represent the formal product of double hydrogen atom addition to the known bis(iminosemiquinone) complexes; interconversions among these species thus open a window into the thermodynamics and kinetics of hydrogen atom transfer processes in strongly coupled diradical complexes.

RESULTS

Preparation of Palladium and Platinum Bis(aminophenoxide) Complexes (^{t}BuClipH_2)M. Attempted metalation of palladium acetate with ^{t}BuClipH_4 gives only the ligand-oxidized iminosemiquinone complex (^{t}BuClip)Pd, even under anaerobic conditions, with $Pd(OAc)_2$ being reduced to palladium black in the process.[16] Once formed and purified, the dark green bis(iminosemiquinone) complex (^{t}BuClip)Pd reacts with hydrazobenzene to form *trans*-azobenzene and the yellow bis(aminophenoxide) complex (^{t}BuClipH_2)Pd (eq 1). In situ monitoring of the reaction by NMR spectroscopy indicates that the reaction is quantitative, but there are significant losses because of the solubility of the product upon isolation. The compound with an unsubstituted 2,2′-biphenylene bridge, (Clip)Pd,[10] reacts analogously.

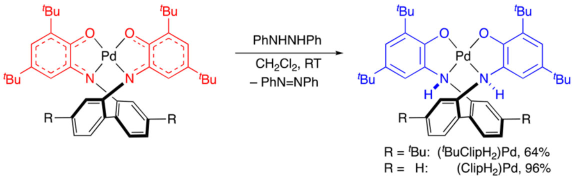

R = ^{t}Bu: (^{t}BuClipH_2)Pd, 64%
R = H: (ClipH_2)Pd, 96%

(1)

The products show the properties expected for square-planar palladium(II) complexes. They are diamagnetic and air-stable, with normal ^1H and ^{13}C NMR spectra, and show essentially no optical absorption at $\lambda > 450$ nm. The presence of the added hydrogen atoms on the amine nitrogen atoms is suggested by NH stretches in IR (3215 cm^{-1}) and N*H* resonances in the ^1H

NMR at δ 5.80. The relatively upfield position of this resonance strongly suggests that the molecule does not form hydrogen-bonded dimers in solution, in contrast to the structurally characterized palladium bis(aminophenoxide) complexes $\{([3,5\text{-}^t\mathrm{Bu}_2\mathrm{C}_6\mathrm{H}_3\mathrm{NH}]\mathrm{C}_6\mathrm{H}_2{}^t\mathrm{Bu}_2\mathrm{O})_2\mathrm{Pd}\}_2$ (with N*H* at δ 8.57)[16] or $\{(\mathrm{CH}_3)_2\mathrm{C}(\mathrm{CH}_2\mathrm{NHC}_6\mathrm{H}_2{}^t\mathrm{Bu}_2\mathrm{O})_2\mathrm{Pd}\}_2$ (with N*H* at δ 7.54).[12]

The 2-fold symmetry shown by the NMR spectra suggests that the compound adopts a C_2-symmetric geometry, which is confirmed by the solid-state structure of $(\mathrm{ClipH}_2)\mathrm{Pd}$ (Table 1 and Figure 1). The molecule crystallizes with a molecule of tetrahydrofuran (THF) hydrogen-bonded to N1−H, which may be the source of the slight asymmetry of the Pd−N distances. In contrast to the bis(iminosemiquinone) complex (Clip)Pd, the 2,2′-biphenylene linker does not induce a significant deviation of the coordination sphere from planarity, with the angle between ligand planes in $(\mathrm{ClipH}_2)\mathrm{Pd}$ of only 2.7° compared to 30.1° in (Clip)Pd.[10] Reduction of the ligand framework does not affect the Pd−O distances significantly but results in a 0.09 Å elongation of the average Pd−N distances [from 1.954(5) Å in (Clip)Pd to 2.040(9) Å in $(\mathrm{ClipH}_2)\mathrm{Pd}$].

Table 1. X-ray Crystallography of $(^t\mathrm{BuClipH}_2)\mathrm{Pd}\cdot\mathrm{C}_4\mathrm{D}_8\mathrm{O}$

empirical formula	$\mathrm{C}_{44}\mathrm{H}_{50}\mathrm{D}_8\mathrm{N}_2\mathrm{O}_3\mathrm{Pd}$
temperature (K)	200(2)
λ (Å)	1.54178 (Cu Kα)
cryst syst	monoclinic
space group	$P2_1/n$
total data collected	66059
no. of indep reflns	7984
R_{int}	0.0461
obsd reflns $[I > 2\sigma(I)]$	7316
a (Å)	9.6206(2)
b (Å)	14.6796(2)
c (Å)	29.2837(4)
α (deg)	90
β (deg)	91.7843(9)
γ (deg)	90
V (Å^3)	4133.63(12)
Z	4
μ (mm^{-1})	3.914
cryst size (mm)	0.17 × 0.12 × 0.05
no. of refined param	606
R indices $[I > 2\sigma(I)]$	R1 = 0.0418, wR2 = 0.1026
R indices (all data)	R1 = 0.0462, wR2 = 0.1049
GOF	1.185

The platinum complex $(^t\mathrm{BuClip})\mathrm{Pt}$ also reacts with hydrazobenzene to form *trans*-azobenzene and $(^t\mathrm{BuClipH}_2)\mathrm{Pt}$, but the reaction is not preparatively useful because it does not go to completion [$K_{\mathrm{eq}} = 0.043(7)$ in CDCl_3; eq 2].

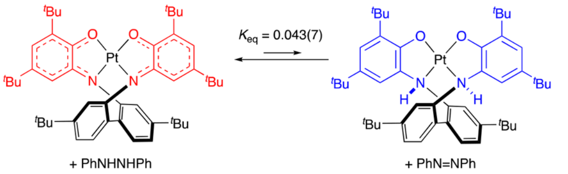

(2)

Synthetically, catalytic hydrogenation over palladium on carbon gives complete reduction and allows the isolation of $(^t\mathrm{BuClipH}_2)\mathrm{Pt}$ in 70% yield (eq 3). No reaction takes place

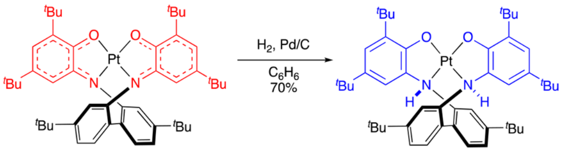

(3)

with H_2 in the absence of the heterogeneous catalyst. In contrast to the palladium analogue, $(^t\mathrm{BuClipH}_2)\mathrm{Pt}$ is quite air-sensitive in solution, rapidly oxidizing to the bis(iminosemiquinone).

Generation of the Mono(iminosemiquinone) Complex $(^t\mathrm{BuClipH})\mathrm{Pd}$. Treatment of a solution of $(^t\mathrm{BuClip})\mathrm{Pd}$ with a large excess of $(^t\mathrm{BuClipH}_2)\mathrm{Pd}$ leads to slow bleaching of the intense band at 967 nm and formation of a new

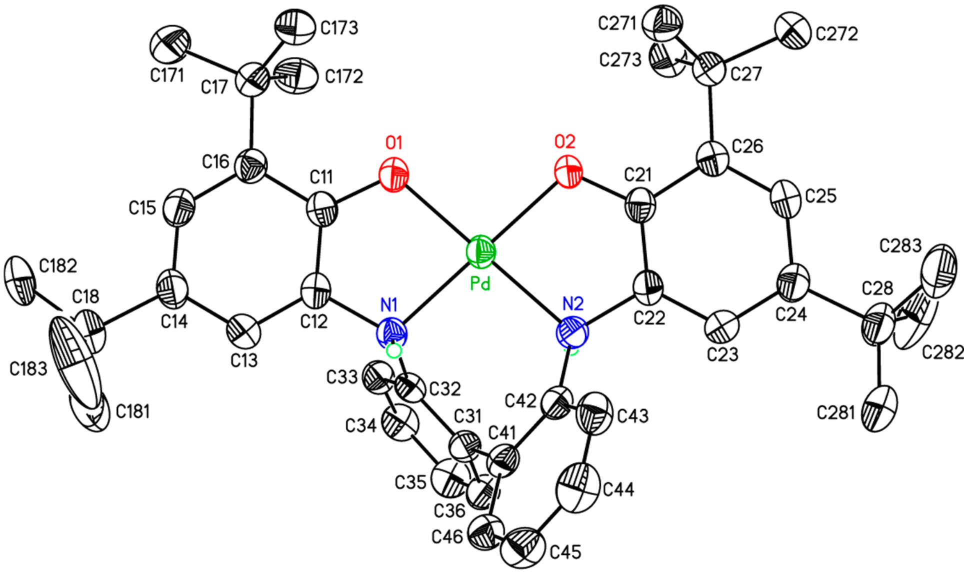

Figure 1. Thermal ellipsoid plot of $(\mathrm{ClipH}_2)\mathrm{Pd}$. Hydrogen atoms (except for the NH hydrogen atoms), lattice THF, and minor components of the disordered *tert*-butyl groups have been omitted for clarity. Selected bond distances (Å): Pd−O1, 1.993(2); Pd−O2, 1.994(2); Pd−N1, 2.033(2); Pd−N2, 2.046(3).

DOI: 10.1021/acs.inorgchem.8b00068
Inorg. Chem. XXXX, XXX, XXX−XXX

chromophore in the near-IR region (Figure 2) as the bis(iminosemiquinone) and bis(aminophenoxide) comproportionate to form the monoaminophenoxide−monoiminosemiquinone complex (^{t}BuClipH)Pd (eq 4). Formation of the monoradical complex is clean, as indicated by the presence of isosbestic points at 488, 498, 530, 588, and 715 nm. The reaction adheres to pseudo-first-order kinetics under these conditions of excess (^{t}BuClipH$_2$)Pd (Figure 2, inset). The observed rate constants generally increase with increasing concentration of (^{t}BuClipH$_2$)Pd, and although reproducibility is mediocre, one can roughly estimate an overall second-order rate constant k_{com} = 0.06 ± 0.02 L mol^{-1} s^{-1} at 23 °C in toluene.

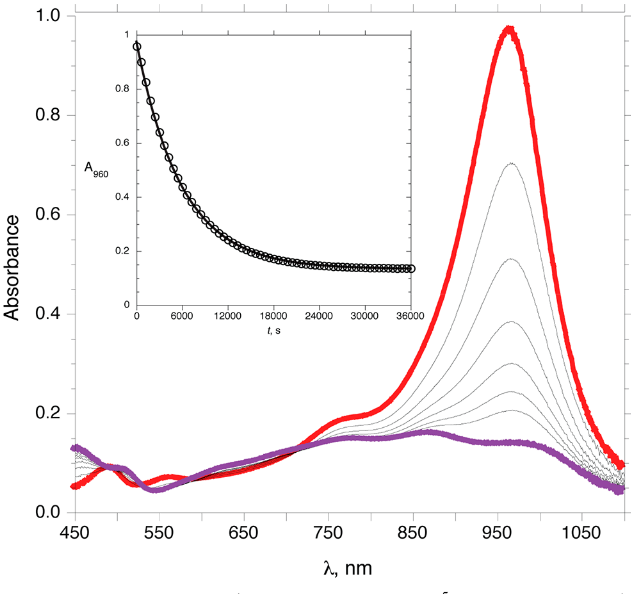

Figure 2. Successive optical spectra of (^{t}BuClip)Pd (2.6 × 10^{-5} M) treated with (^{t}BuClipH$_2$)Pd (2.0 × 10^{-3} M). The initial spectrum is solid red, and subsequent spectra are at 2400 s intervals, with the final spectrum (solid purple) at t = 36000 s. Inset: A_{960} as a function of time. The solid line is the best fit to first-order decay.

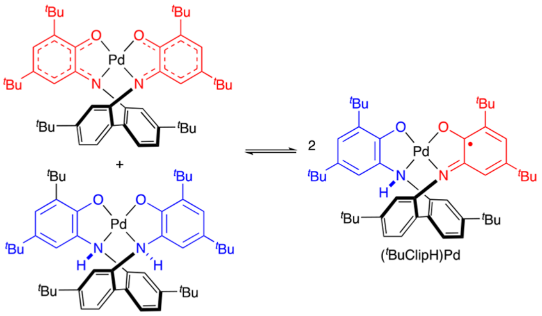

(4)

The product (^{t}BuClipH)Pd has not been isolated, but its spectroscopic features unequivocally support its assignment as a monoiminosemiquinone complex. In particular, the optical spectrum of the equilibrium reaction mixture in the presence of excess (^{t}BuClipH$_2$)Pd, with its structured, long-wavelength (λ_{max} = 869 nm) transition with a vibronic progression with a spacing of ∼1250 cm^{-1}, is extremely similar to those of other well-characterized neutral palladium mono(iminosemiquinone) complexes prepared by van der Vlugt and co-workers.[19−21] Cationic [(ISQ)Pd(bpy)]$^+$ has a similar band.[11] The fluid solution, ambient-temperature electron paramagnetic resonance (EPR) spectrum of the reaction mixture (Figure 3) is likewise characteristic of an organic iminosemiquinone radical (g = 2.0037), with hyperfine couplings observable to nitrogen, hydrogen, and palladium nuclei. It is very similar to spectra previously observed for other neutral palladium monoiminosemiquinones[20−22] and is nearly superimposable on that shown by (^{t}Bu$_2$C$_6$H$_2$ONCMe$_2$C$_5$H$_4$N)Pd(N$_3$).[19]

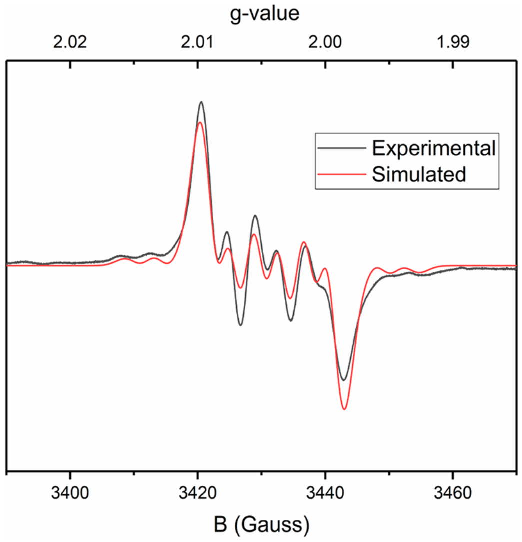

Figure 3. X-band EPR spectrum of (^{t}BuClipH)Pd, generated in situ by comproportionation of (^{t}BuClipH$_2$)Pd and (^{t}BuClip)Pd (toluene, 296 K). Simulated hyperfine coupling constants: A_N = 21.8 MHz, $A_{H\text{-}5}$ = −10.6 MHz, $A_{H\text{-}3}$ = −3.0 MHz, and A_{Pd} = 13.2 MHz.

When mixtures of (^{t}BuClip)Pd and (^{t}BuClipH$_2$)Pd are examined by NMR, the signals of the two compounds remain distinct and unshifted. Their intensities decrease (relative to an internal standard) over time but do not go to zero, indicating that comproportionation (eq 4) is not strongly favored thermodynamically. The signals for the aromatic hydrogen atoms of the odd-electron complex (^{t}BuClipH)Pd are apparently too broad to be observed, although a broadened signal, presumably due to a *tert*-butyl group, is observed at 2.0 ppm. By measuring the decrease in the signal intensity of the diamagnetic compounds compared to the internal standard at equilibrium, one can measure a value of K_{com} = 1.9 ± 0.3 in CDCl$_3$.

In contrast to the palladium analogue, there is no evidence for appreciable comproportionation of (^{t}BuClip)Pt with (^{t}BuClipH$_2$)Pt. The optical spectrum of (^{t}BuClip)Pt is unchanged upon treatment with (^{t}BuClipH$_2$)Pt; significant changes would have been expected because platinum monoiminosemiquinones have spectral features similar to those of their palladium analogues.[23] The NMR spectral intensities and chemical shifts of the two compounds are also unchanged upon mixing. Comproportionation is thus concluded to be thermodynamically unfavorable in the case of the platinum complexes, with K_{com} < 0.1.

Thermodynamics of Hydrogenation of (^{t}BuClip)M. The platinum bis(iminosemiquinone) complex (^{t}BuClip)Pt reacts reversibly with hydrazobenzene to give azobenzene (eq 2), giving $\Delta G°_2$ = +1.85 kcal mol^{-1}. The average bond dissociation free energy (BDFE) of hydrazobenzene, upon dehydrogenation to give *trans*-azobenzene as its product, is 59.6

kcal mol^{-1}, based upon its solution enthalpy of reaction with excess 2,4,6-tri-*tert*-butylphenoxyl radical (BDFE = 76.7 kcal mol^{-1})[8] of −34.27 kcal mol^{-1} in C_6H_6[24] and neglecting entropy changes in the reaction of the aroxyl radical with hydrazobenzene, which appears to be reasonable in organic hydrogen atom transfer reactions.[25] This implies that the average BDFE for the two N−H bonds in (^{t}BuClipH$_2$)Pt is 58.6 kcal mol^{-1} (Scheme 1). The fact that comproportionation of (^{t}BuClipH$_2$)Pt and (^{t}BuClip)Pt is thermodynamically unfavorable, with K_{com} < 0.1, implies that the BDFE of an N−H bond in (^{t}BuClipH$_2$)Pt must be greater than that of the N−H bond in putative (^{t}BuClipH)Pt by at least 1.3 kcal mol^{-1}.

Scheme 1. Determination of the Average N−H BDFEs of Hydrazobenzene and (^{t}BuClipH$_2$)Pt

$$\begin{array}{rr}
2\ \text{ArO–H} \rightarrow 2\ \text{ArO}\bullet\ +\ 2\ \text{H}\bullet & \Delta G^\circ = 2\times(\text{BDFE}_{\text{O–H}}) = 153.4\ \text{kcal mol}^{-1} \\
\text{PhNHNHPh} + 2\ \text{ArO}\bullet \rightarrow \text{PhN=NPh} + 2\ \text{ArOH} & \Delta G^\circ \approx \Delta H^\circ = -34.3\ \text{kcal mol}^{-1} \\
\hline
\text{PhNHNHPh} \rightarrow \text{PhN=NPh} + 2\ \text{H}\bullet & \Delta G^\circ = 2\times(\text{avg. N-H BDFE}) = 119.1\ \text{kcal mol}^{-1} \\
 & \therefore\ \textbf{Avg. N-H BDFE in PhNHNHPh = 59.6 kcal mol}^{-1}
\end{array}$$

$$\begin{array}{rr}
(^t\text{BuClipH}_2)\text{Pt} + \text{PhN=NPh} \rightarrow (^t\text{BuClip})\text{Pt} + \text{PhNHNHPh} & \Delta G^\circ = -RT\ln(K_{eq}) = -1.85\ \text{kcal mol}^{-1} \\
\text{PhNHNHPh} \rightarrow \text{PhN=NPh} + 2\ \text{H}\bullet & \Delta G^\circ = 119.1\ \text{kcal mol}^{-1} \\
\hline
(^t\text{BuClipH}_2)\text{Pt} \rightarrow (^t\text{BuClip})\text{Pt} + 2\ \text{H}\bullet & \Delta G^\circ = 2\times(\text{avg. N-H BDFE}) = 117.3\ \text{kcal mol}^{-1} \\
 & \therefore\ \textbf{Avg. N-H BDFE in (}^t\textbf{BuClipH}_2\textbf{)Pt = 58.6 kcal mol}^{-1}
\end{array}$$

The reaction of hydrazobenzene with the palladium complex (^{t}BuClip)Pd (eq 1) goes to completion. Qualitatively, this indicates that the N−H bonds in (^{t}BuClipH$_2$)Pd are significantly stronger than those in its platinum analogue. In order to make a quantitative estimate of the strength of the N−H bonds in the palladium complex, a weaker reductant than PhNHNHPh is required in order to allow the reaction to go to a measurable equilibrium. This was achieved using 4,4′-dinitrohydrazobenzene (eq 5), where NMR monitoring of the reaction between (^{t}BuClipH$_2$)Pd and $O_2NC_6H_4N{=}NC_6H_4NO_2$ (in THF-d_8, due to the very low solubility of nitrohydrazobenzene in aromatic solvents) gives K_5 = 0.89(3).

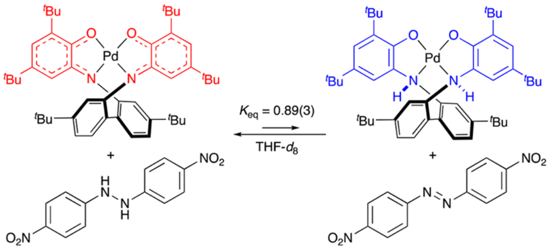

(5)

In order to compare the BDFE of the palladium complex to that of the platinum complex, one needs to be able to compare the thermodynamics of the azobenzene/hydrazobenzene couple to that of the 4,4′-dinitroazobenzene/4,4′-dinitrohydrazobenzene couple. This was done by constructing a thermodynamic ladder, whereby successively more strongly oxidizing azoarenes were allowed to equilibrate with more reducing hydrazoarenes. These reactions (eq 6) were found to come to equilibrium in THF-d_8 within 2 days in the presence of solid palladium on carbon as a catalyst. By interposing several different intermediary levels of oxidizing power, one can indirectly determine the difference in the average BDFEs between hydrazobenzene and 4,4′-dinitrohydrazobenzene as 3.56 kcal mol^{-1} (Table 2). Combined with the value of K_5 and the average BDFE in hydrazobenzene, this gives an average BDFE for the N−H bonds in (^{t}BuClipH$_2$)Pd of 63.1 kcal mol^{-1} (Figure 4). Using the value of $\Delta G°_{com}$ determined in $CDCl_3$, −0.38(9) kcal mol^{-1}, one may conclude that breaking an N−H bond in (^{t}BuClipH$_2$)Pd requires slightly less free energy (62.9 kcal mol^{-1}) than breaking the N−H bond in (^{t}BuClipH)Pd (63.3 kcal mol^{-1}).

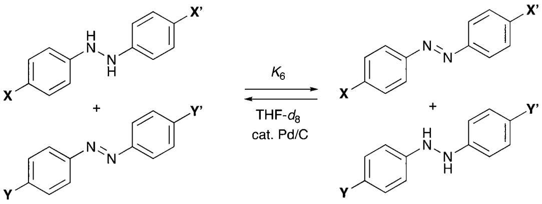

(6)

Table 2. Relative Reducing Ability of Substituted Hydrazobenzenes

X, X′	Y, Y′	K_6	average N−H BDFE in $YC_6H_4NHNHC_6H_4Y'$, relative to Y = Y′ = H (kcal mol^{-1})
H, H	H, H	1.00	0.00
H, H	Br, Br	6.3(5)	0.54
Br, Br	H, NO$_2$	64(7)	1.77
H, NO$_2$	CO$_2$CH$_3$, CO$_2$CH$_3$	1.90(5)	1.95
CO$_2$CH$_3$, CO$_2$CH$_3$	CN, CN	13.2(7)	2.71
CN, CN	NO$_2$, NO$_2$	17.6(4)	3.56

Kinetics of Hydrogen Atom Transfer Reactions of (^{t}BuClipH$_2$)M with Oxygen Radicals. In order to assess the kinetic reactivity of the N−H bonds in the bis(aminophenoxide) complexes, we assayed their reactions with various nitroxyl and aroxyl radicals (Scheme 2). These radicals are all stable monomers in solution, and the corresponding O−H compounds span a range of about 11 kcal mol^{-1} in BDFE (Table 3). In all cases, reactions of an excess (>2 equiv) of reagent with (^{t}BuClipH$_2$)M resulted in the quantitative formation of (^{t}BuClip)M by NMR. These reagents are known to have a strong predilection for single hydrogen atom transfer reactions; as one-electron oxidants, they are not capable of removing both hydrogen atoms simultaneously from (^{t}BuClipH$_2$)M. The reactions thus presumably involve an initial hydrogen atom transfer to form (^{t}BuClipH)M, followed by a second hydrogen atom transfer to form the final product (^{t}BuClip)M.

In the case of M = Pd, the observed reaction traces with most oxidants display discernibly biphasic kinetics (Figure 5), with an initially accelerating phase in the growth of A_{960}, where (^{t}BuClip)Pd absorbs strongly (Figure 2; ε = 37500 L mol^{-1} cm^{-1} in toluene) and (^{t}BuClipH)Pd absorbs only modestly (ε = 3600 L mol^{-1} cm^{-1}). The data can be fit to successive irreversible pseudo-first-order reactions[26] using known extinction coefficients to determine $k_{1(obs)}$ and $k_{2(obs)}$. In all cases, k_1 is observed to be somewhat faster than k_2. On the basis of the low concentrations of palladium and the relatively slow kinetics measured earlier, comproportionation/disproportionation reactions cannot contribute significantly to the time evolution of the palladium species; comproportionation would take place on the time scale of hundreds of hours under these conditions, and even the slowest of the reactions is complete in under 5 h. Therefore, k_1 is assigned to hydrogen atom transfer from (^{t}BuClipH$_2$)Pd to the oxyl radical, while k_2 is assigned to

DOI: 10.1021/acs.inorgchem.8b00068
Inorg. Chem. XXXX, XXX, XXX−XXX

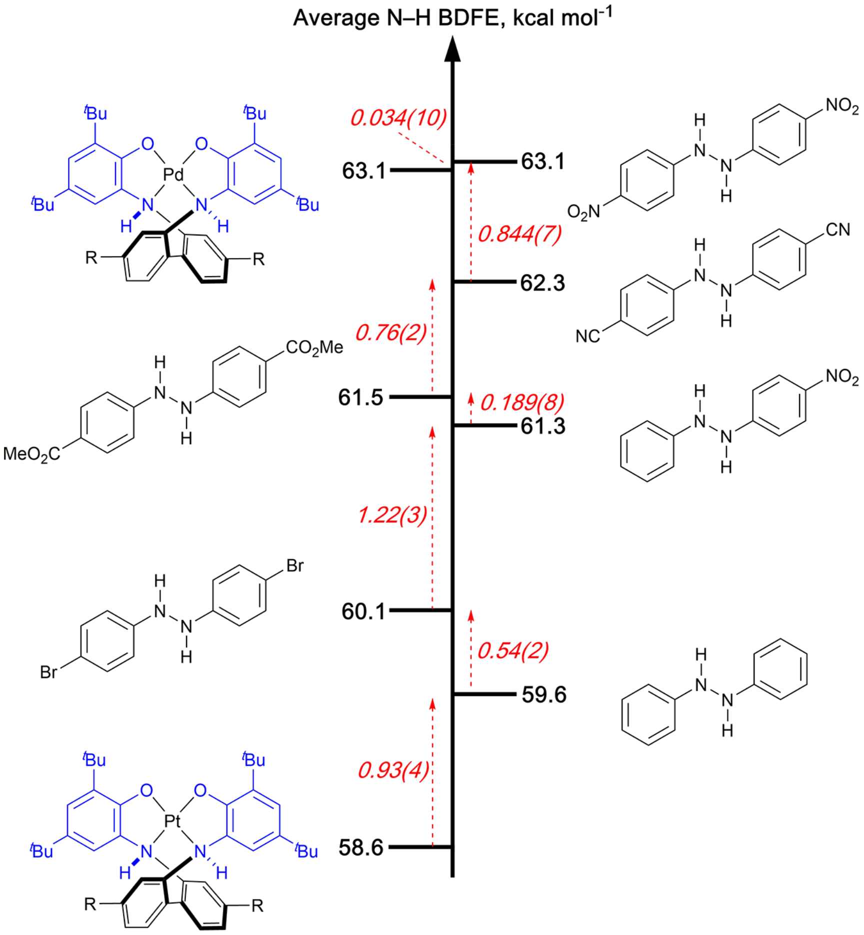

Figure 4. Thermodynamic ladder connecting (^{t}BuClipH$_2$)Pd to (^{t}BuClipH$_2$)Pt via intermediary substituted hydrazobenzenes. The values in bold are the average N−H BDFE (kcal mol^{-1} at 296 K) for the indicated compound. Italicized values in red are measured differences in free energy based on measurement of the equilibrium of eq 2, eq 5, or eq 6, with ΔBDFE = $-0.5 \times RT \ln(K_{eq})$. The factor of 0.5 arises because two N−H bonds are broken and formed in each equilibrium.

Scheme 2. Reactions of Oxygen Radicals with (^{t}BuClipH$_2$)M (M = Pd, Pt)

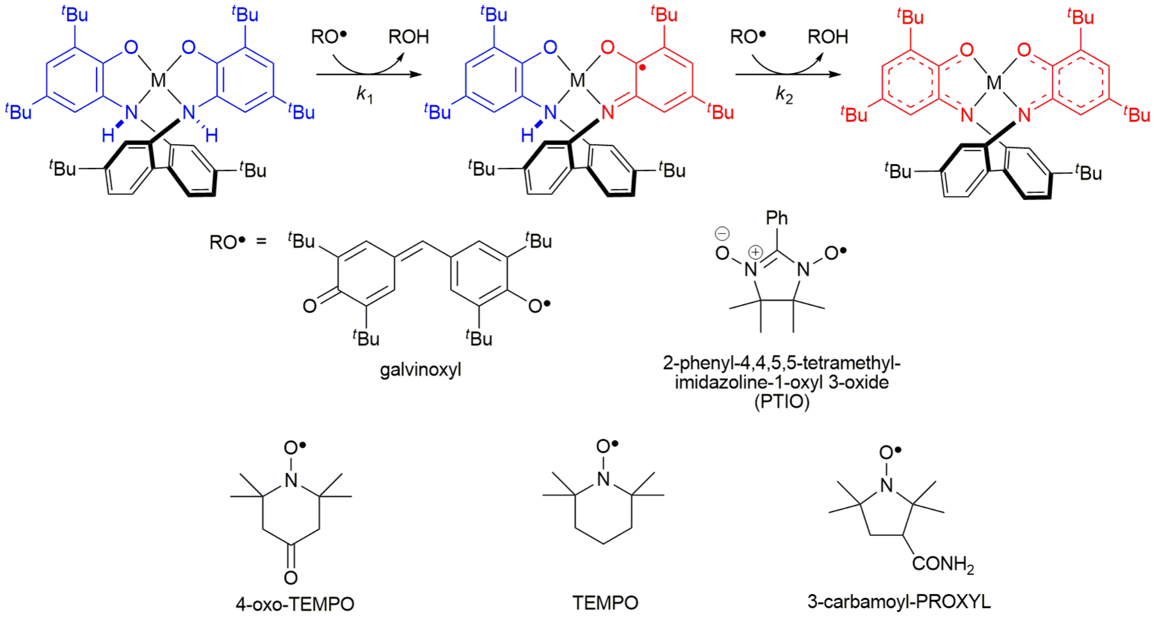

hydrogen atom transfer from the intermediate (^{t}BuClipH)Pd to the oxyl radical.

In the reactions of (^{t}BuClipH$_2$)Pt, only monophasic kinetics, to form fully oxidized (^{t}BuClip)Pt, are observed (Figure 6).

Table 3. Kinetics of Reactions of (^{t}BuClipH$_2$)M (M = Pd, Pt) with Oxygen Radicals

radical RO$^\bullet$	BDFE of RO−H (kcal mol^{-1})[a]	ref for BDFE	k_1{Pd} (L mol^{-1} s^{-1})	k_2{Pd} (L mol^{-1} s^{-1})	k_1{Pt} (L mol^{-1} s^{-1})
galvinoxyl	74.1	27	228(5)	n.d.	745(10)
PTIO	67.5	28[b]	940(30)	207(6)	2390(80)
4-oxo-TEMPO	65.6	29[c]	38.5(9)	14.6(2)	78(4)
TEMPO	65.1	30	41.7(20)	12.70(16)	90.2(18)
3-carbamoyl-PROXYL	63.3	31[b]	2.77(6)	1.64(2)	8.46(5)

[a] Determined in benzene or toluene, except as noted. Anchored to the value of 76.7 kcal mol^{-1} for 2,4,6-tri-*tert*-butylphenoxyl in C_6H_6.[8] [b] Based on aqueous electrochemistry, corrected to C_6H_6 based on the difference between the aqueous and C_6H_6 BDFEs of TEMPO-H. [c] Based on equilibration between 4-oxo-TEMPO and TEMPO-H in heptane.

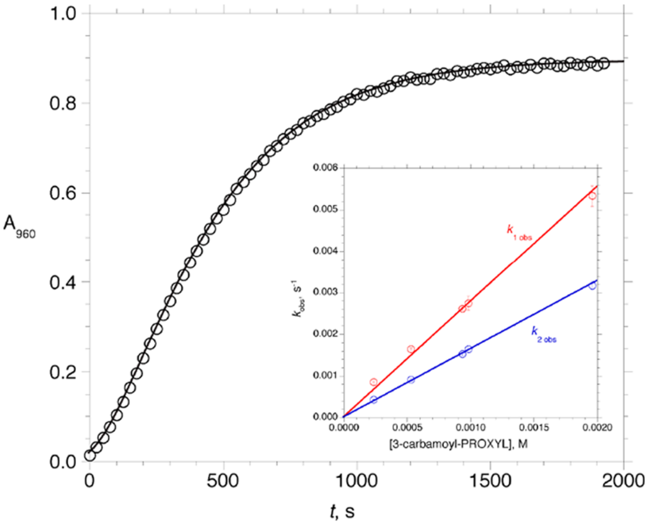

Figure 5. Absorbance (at 960 nm) versus time for the reaction of (^{t}BuClipH$_2$)Pd (2.3×10^{-5} M) with 3-carbamoyl-PROXYL (2.0×10^{-3} M) (toluene, 23 °C). The curve is fit to successive irreversible pseudo-first-order reactions. Inset: k_{obs} versus [3-carbamoyl-PROXYL].

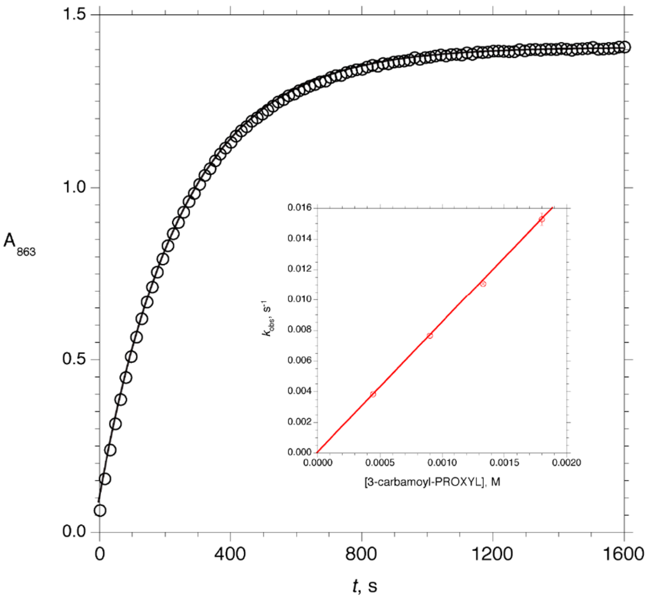

Figure 6. Absorbance (at 863 nm) versus time for the reaction of (^{t}BuClipH$_2$)Pt (2×10^{-5} M) with 3-carbamoyl-PROXYL (4.4×10^{-4} M) (toluene, 23 °C). The curve is fit to a simple pseudo-first-order reaction. Inset: k_{obs} versus [3-carbamoyl-PROXYL].

Given the ligand-localized structure of the monoiminosemiquinone complex (in the case of palladium), one would expect (^{t}BuClipH)Pt to show similar spectroscopic features, and no such spectral signatures (such as long-wavelength absorption) are observed at any point in the reaction. The conclusion is thus that the monoradical complex (^{t}BuClipH)Pt does not accumulate to a significant extent. Presumably, the oxygen radical reacts substantially more rapidly (by at least a factor of 10) with (^{t}BuClipH)Pt than it does with (^{t}BuClipH$_2$)Pt, with k_{obs} corresponding to the initial hydrogen atom transfer from (^{t}BuClipH$_2$)Pt. The reaction of the palladium complex with galvinoxyl also shows monophasic kinetics.

In all cases, varying the concentration of the oxidant results in proportionate increases in all of the observed pseudo-first-order rate constants, consistent with identification of the reactions as overall second order (first order in both the oxidant and aminophenoxide complex). The second-order rate constants are compiled in Table 3.

■ DISCUSSION

Thermodynamics of Hydrogen Atom Transfer of Palladium and Platinum Bis(iminosemiquinone) Complexes. The bis(iminosemiquinone) complexes of group 10 metals are generally considered to have a central metal(II) ion bonded to ligand-localized radicals; accessible redox reactions are invariably assigned to ligand-centered reductions or oxidations.[13] Binding to the metal has a significant impact on the properties of the aminophenoxide/iminosemiquinone redox couple. The free organic aminophenol 4,6-di-*tert*-butyl-2-(*tert*-butylamino)phenol has a BDFE of 76.7 kcal mol^{-1}.[32] Metal coordination greatly stabilizes the iminosemiquinone relative to the aminophenol, weakening the N−H BDFEs of the palladium- and platinum-bound aminophenoxides by 15−20 kcal mol^{-1}.

The nature of the metal also has a significant thermodynamic impact: the palladium(II) complex (^{t}BuClip)Pd is some 8.9 kcal mol^{-1} better able to abstract the elements of H_2 than is the platinum(II) complex (^{t}BuClip)Pt (eq 7), as measured

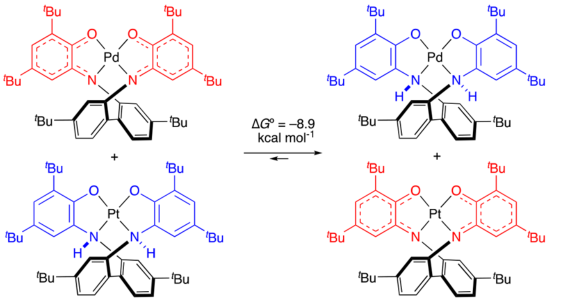

(7)

experimentally via the thermodynamic ladder connecting the two compounds (Figure 4). The difference is qualitatively evident in their reactions with hydrazobenzene, as (^{t}BuClip)Pd oxidizes hydrazobenzene irreversibly to *trans*-azobenzene, while (^{t}BuClip)Pt only oxidizes hydrazobenzene to a small extent at equilibrium.

Upon reflection, it makes sense that the metal should exert a significant influence on the thermodynamics even of a nominally ligand-localized reaction. It is well appreciated that ancillary ligands can have dramatic effects on the metal-centered reactivity, so it should not be too surprising that ancillary metals can have dramatic effects on ligand-centered reactivity. Spectroscopic studies indicate that the bonding interactions in these bis(iminosemiquinone) complexes are markedly stronger for the platinum complexes than for the palladium complexes, with the differences in the energies of the metal−ligand nonbonding and antibonding orbitals increasing from 4800 cm^{-1} in (^{t}BuClip)Pd to 6300 cm^{-1} in (^{t}BuClip)Pt (a difference of 4.2 kcal mol^{-1}).[16] Reduction of the iminosemiquinones results in increased occupation of the metal−ligand π antibonding orbitals, which is more costly for the platinum complexes, thus decreasing the relative stability of the hydrogenated bis(aminophenoxide) complexes. This trend is evident in the redox potentials of the complexes, where the (^{t}BuClip)M$^{0/-}$ redox potential is 80 mV more positive for palladium and the (^{t}BuClip)M$^{-/2-}$ redox potential is 220 mV more positive. This 150 mV (average) difference translates to a 3.5 kcal mol^{-1} difference in the average BDFEs, accounting for most of the 4.5 kcal mol^{-1} total difference. The balance of the difference must be due to the palladium anions being more basic than the platinum anions, which may be due to stronger metal−nitrogen σ bonding in the platinum compounds.

Computationally, eq 7 has been analyzed using density functional theory (DFT), using the B3LYP and SDD basis sets for palladium and platinum and a 6-31G* basis set for other atoms, on gas-phase molecules with all of the *tert*-butyl groups replaced by hydrogen atoms. The computed value for $\Delta G°_7$, −8.7 kcal mol^{-1}, agrees exceptionally well with the experimental value of −8.9 kcal mol^{-1}. The good agreement is surprising because the strongly multireference character of the bis(iminosemiquinone) complexes[15] does not inspire confidence that their energetics could be accurately modeled using a B3LYP functional. It is possible that some fortuitous cancellation of errors in the descriptions of the two bis(iminosemiquinone) complexes in eq 7 contributes to the apparent accuracy of the DFT methods. This cannot, however, be the full explanation because computations on the reactions of bis(iminosemiquinones) with hydrazoarenes (eqs 2 and 5), where only a single reagent has significant multireference character, also give good results. The agreement of the calculated values ($\Delta G°_2$ = 0.9 kcal mol^{-1}; $\Delta G°_5$ = −2.1 kcal mol^{-1}) with the experimental values (1.8 and 0.1 kcal mol^{-1}, respectively) is not as sparkling as the agreement on eq 7 but is still quite reasonable. We therefore conclude that the DFT/B3LYP method is remarkably tenable for computing the energetics of reactions involving these bis(iminosemiquinone) complexes.

Thermodynamic and Kinetic Coupling between the N−H Bonds in (^{t}BuClipH$_2$)M. Qualitatively, there is a striking contrast between the two metals in the degree of communication between the N−H bonds in the bis(aminophenoxide) complexes (^{t}BuClipH$_2$)M. In the palladium complex, the two N−H bonds appear to act essentially independently of one another. Comproportionation between (^{t}BuClipH$_2$)Pd and (^{t}BuClip)Pd takes place readily, with the equilibrium constant for comproportionation K_{com} not too different from the statistical value of 4 expected if the two bonds were completely independent of one another. Kinetically, a comparison of the rate constants for the reaction with nitroxyl radicals of (^{t}BuClipH$_2$)Pd to those of (^{t}BuClipH)Pd shows that the fully reduced compound enjoys a kinetic advantage not too different from the factor of 2 expected on statistical grounds.

The situation is quite different for the platinum complexes. Comproportionation of (^{t}BuClipH$_2$)Pt with (^{t}BuClip)Pt is not observed, and only single-exponential decay is observed in the reactions of (^{t}BuClipH$_2$)Pt with oxygen radicals, consistent with the presumed intermediate (^{t}BuClipH)Pt having much greater kinetic reactivity than the fully reduced compound. In other words, both thermodynamically and kinetically, removal of the first hydrogen atom from (^{t}BuClipH$_2$)Pt greatly weakens the remaining N−H bond; the two ligands do not behave independently.

One can make a quantitative estimate of the thermodynamic separation in the N−H bond strength of the two N−H bonds using the observed kinetics. The rates of reaction of the aminophenoxide complexes with oxygen radicals are clearly correlated with the BDFEs of the O−H bonds being formed (Figure 7): as the driving force for atom transfer increases, the activation energy for atom transfer decreases. This kind of Evans−Polanyi relationship is widely observed in hydrogen atom transfer reactions.[1,33] The correlation is good for all of the nitroxyl radicals, but the reactions with galvinoxyl are much slower than expected based on this correlation, possibly because of the greater bulk of the galvinoxyl radical. The lines relating the reactions of (^{t}BuClipH$_2$)M with the nitroxyl

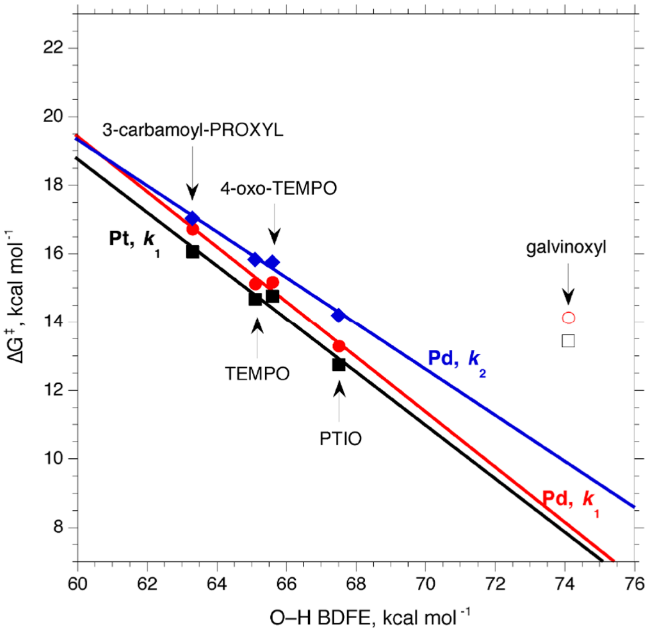

Figure 7. Correlation of the free energies of activation for the abstraction of N−H bonds with the BDFEs of the formed O−H bonds of the abstracting oxygen radicals: reaction of (^{t}BuClipH$_2$)Pd, red circles; reaction of (^{t}BuClipH)Pd, blue diamonds; reaction of (^{t}BuClipH$_2$)Pt, black squares. Open symbols represent the reactions with galvinoxyl and were not used in the correlation.

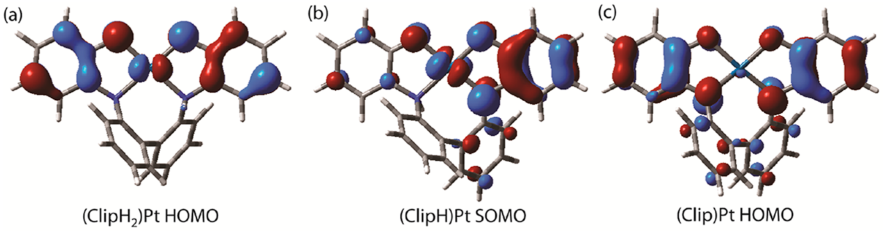

Figure 8. Frontier Kohn−Sham orbitals of (Clip)Pt species. (a) Highest occupied molecular orbital of (ClipH$_2$)Pt. (b) Singly occupied molecular orbital of (ClipH)Pt. (c) Highest occupied molecular orbital of (Clip)Pt.

radicals are essentially parallel [slope for M = Pd, −0.80(8); slope for M = Pt, −0.78(10)], while the reaction of (^{t}BuClipH)Pd with the oxygen radicals is perhaps slightly less sensitive to the driving force of the reaction [slope = −0.67(5)].

The observation of good correlations between the reaction rates of the nitroxyl radicals and the reactions' driving force indicates that differences in the rate of reaction are largely determined by differences in the bond strengths of the bonds being broken and formed. This explanation may plausibly be extended to explain the differences in reactivity between the palladium and platinum complexes; that is, it is likely that the faster rate of reaction of the oxygen radicals with (^{t}BuClipH$_2$)Pt compared to its palladium congener is due to the weaker N−H bond in the platinum complex. In this case, one can use the observed kinetic correlations to estimate the difference in the bond strengths for the scissile N−H bonds in the two compounds. For the five reactions studied, $\Delta\Delta G^{\ddagger}$ for reactions of (^{t}BuClipH$_2$)Pd compared to those of (^{t}BuClipH$_2$)Pt [corresponding to $-RT\ \ln(k_1\{\text{Pd}\}/k_1\{\text{Pt}\})$] averages 0.55 ± 0.12 kcal mol^{-1}. Given the slope of the Evans−Polanyi plot in Figure 6 of about −0.8, this corresponds to a difference in the driving force $\Delta\Delta G°$ = 0.70 ± 0.15 kcal mol^{-1}, with the reaction of the platinum compound more exergonic than that of the palladium compound. Given a BDFE of 62.9 kcal mol^{-1} for an N−H bond in (^{t}BuClipH$_2$)Pd, this implies a BDFE of 62.2 kcal mol^{-1} for an N−H bond in (^{t}BuClipH$_2$)Pt. Given the average BDFE in the platinum complex of 58.6 kcal mol^{-1}, this means that the BDFE of the N−H bond in (^{t}BuClipH)Pt is only 55.1 kcal mol^{-1}, 7.1 kcal mol^{-1} weaker than the first N−H bond. This corresponds to a K_{com} of 6×10^{-6} for the comproportionation of (^{t}BuClipH$_2$)Pt with (^{t}BuClip)Pt, consistent with the unobservability of the monoradical complex (^{t}BuClipH)Pt. On the basis of these thermodynamics, the correlation in Figure 7 predicts that (^{t}BuClipH)Pt would react with nitroxyl radicals ~10^4 times faster than (^{t}BuClipH$_2$)Pt would, consistent with the observation of simple pseudo-first-order kinetics in these reactions.

One possible reason for the platinum complex to shun the monoradical is that it presents a uniquely unfavorable π-bonding arrangement. The singly occupied π orbital in the iminosemiquinone (the so-called redox-active orbital) is relatively high in energy because of its C−O and C−N antibonding character and therefore interacts strongly with the metal dπ orbitals. In contrast, the filled ligand-centered π orbital in the fully reduced aminophenoxide ligand is mostly oxygen in character and is C−O nonbonding, hence lower in energy, and so experiences a weaker antibonding interaction with the filled dπ orbitals (Figure 8a). In the monoiminosemiquinone, the ligand redox-active orbital is singly occupied and must be metal−ligand antibonding (Figure 8b). In contrast, in the bis(iminosemiquinone) complexes, one combination of the ligand redox-active orbitals has essentially no overlap with any of the metal d orbitals (Figure 8c);[11] population of this orbital by the two ligand-centered electrons avoids antibonding interactions.

These concerns will be more pressing for platinum than for palladium. Spectroscopic studies establish that the difference in energy between the nonbonding and antibonding combinations in (^{t}BuClip)M are larger for platinum (6300 cm^{-1}) than palladium (4800 cm^{-1}),[16] and presumably this difference carries over to the antibonding interaction in (^{t}BuClipH)M as well. Because of the modest difference in energy between the nonbonding and metal−ligand π* combinations of the redox-active orbitals, both are significantly occupied in the open-shell singlet ground states of the bis(iminosemiquinone) complexes. However, the greater energy difference for platinum means that there is less occupancy of the antibonding orbital, further enhancing the energetic advantage of the bis(iminosemiquinone) oxidation state for platinum.

It is thus not surprising that the platinum compound should show greater coupling than the palladium compound in its hydrogen atom transfer reactions, but it is surprising that the palladium compound shows essentially no coupling at all. The palladium bis(iminosemiquinone) (^{t}BuClip)Pd, with its singlet−triplet gap of 1940 cm^{-1},[16] shows very strong coupling between the two ligand radicals. Yet this does not seem to transfer over to its behavior in hydrogen atom transfer reactions; only small differences from the behavior expected on the basis of pure statistics are observed. Where (^{t}BuClip)Pd acts like a pair of ligand radicals, the iminosemiquinones in (^{t}BuClip)Pt act as a single entity, with two-electron chemistry strongly favored over one-electron chemistry. Why this cooperation is turned on for platinum but essentially absent for palladium is unclear.

■ CONCLUSIONS

A diradical is not just two radicals; interactions between the two radicals, mediated, for example, by a transition metal, can make a strongly coupled diradical an entity with unique properties. The group 10 bis(iminosemiquinonate) complexes (^{t}BuClip)M (M = Pd, Pt) are excellent candidates to examine whether the very strong coupling evident spectroscopically in both compounds transfers to their reactivity. In hydrogen atom transfer reactions, the two compounds behave markedly differently. The palladium compound readily comproportionates with the reduced (^{t}BuClipH$_2$)Pd to form (^{t}BuClipH)Pd, and in hydrogen atom transfer reactions, the first hydrogen atom is removed from (^{t}BuClipH$_2$)Pd only slightly faster than the second hydrogen atom. These patterns are consistent with the two ligand radicals acting essentially independently of one another, both thermodynamically and kinetically. In contrast, no comproportionation is ever observed with the platinum

DOI: 10.1021/acs.inorgchem.8b00068
Inorg. Chem. XXXX, XXX, XXX−XXX

complexes, and removal of the first hydrogen atom from (^{t}BuClipH$_2$)Pt is much slower than removal of the second hydrogen atom. Using linear free-energy correlations of the reaction rates with driving forces, one can estimate that the second N−H bond is 7.1 kcal mol^{-1} weaker than the first, giving the platinum compound a strong thermodynamic propensity toward two-electron chemistry. Both the attenuated oxidizing power of the platinum compound ($\Delta\Delta G°$ for hydrogenation = 8.9 kcal mol^{-1}) and its greater tendency to disproportionate from the monoradical state are due to stronger metal−ligand π interactions in the platinum compound.

■ EXPERIMENTAL SECTION

Unless otherwise noted, procedures were carried out under a nitrogen atmosphere using glovebox or vacuum-line techniques. NMR spectra were measured on a Bruker Avance DPX 400 or 500 spectrometer. Chemical shifts for ^{1}H and ^{13}C{^{1}H} NMR spectra are reported in ppm downfield of tetramethylsilane, with spectra referenced using the known chemical shifts of the solvent residuals. IR spectra were measured on a Jasco 6300 Fourier transform infrared spectrometer as powders on attenuated-total-reflectance plates. UV−visible−NIR spectra were recorded in 1 cm quartz cells on a ThermoFisher Evolution Array spectrophotometer. Elemental analyses were performed by M-H-W Laboratories (Phoenix, AZ). The bis(iminosemiquinone) complexes (^{t}BuClip)M (M = Pd, Pt)[16] and (Clip)Pd[10] were prepared by literature procedures.

(^{t}BuClipH$_2$)Pd. In the drybox, 0.1235 g of (^{t}BuClip)Pd (0.153 mmol) and 0.0616 g of hydrazobenzene (0.344 mmol) were added to a 25 mL round-bottomed flask and dissolved in 6 mL of dichloromethane to give a dark-green solution. The solution was stirred for 1.5 h on a stir plate to give a yellow solution. The solution was opened to the air and the solvent removed using a rotary evaporator. The yellow residue was slurried in 3 mL of acetonitrile, collected via vacuum filtration on a fine-porosity fritted funnel, and washed with 3 mL of acetonitrile. The product was then air-dried for 15 min to yield 0.0796 g of (^{t}BuClipH$_2$)Pd as orange crystals (64%). ^{1}H NMR (CDCl$_3$): δ 1.17, 1.30, 1.43 (s, 18H each, ^{t}Bu), 5.80 (s, 2H, N*H*), 6.48 (d, *J* = 2.1 Hz, 2H, H-3), 7.04 (d, *J* = 2.2 Hz, 2H, H-5), 7.26 (d, *J* = 7.9 Hz, 2H, H-6′), 7.28 (d, *J* = 1.5 Hz, 2H, H-3′), 7.39 (dd, *J* = 7.9 and 1.8 Hz, 2H, H-5′). ^{13}C{^{1}H} NMR (CDCl$_3$): δ 29.72, 31.38, 32.00 (C(*C*H$_3$)$_3$), 34.19, 35.40, 35.60 (*C*(CH$_3$)$_3$), 116.52, 119.59, 123.55, 123.65, 124.68, 126.39, 130.85, 136.58, 140.20, 145.30, 154.48, 166.89 (CO). IR (cm^{-1}): 3215 (w, ν_{NH}), 2952 (m), 2864 (w), 1617 (w), 1600 (w), 1562 (w), 1469 (m), 1441 (m), 1410 (m), 1362 (m), 1300 (m), 1261 (s), 1203 (m), 1163 (w), 1117 (w), 1023 (w), 1000 (m), 974 (w), 897 (m), 874 (m), 820 (s), 728 (s), 687 (m). Anal. Calcd for $C_{48}H_{66}N_2O_2Pd$: C, 71.22; H, 8.22; N, 3.46. Found: C, 71.02; H, 8.11; N, 3.53.

(ClipH$_2$)Pd. Using the procedure for preparing (^{t}BuClipH$_2$)Pd, 0.1872 g of (Clip)Pd (0.269 mmol) and 0.1024 g of hydrazobenzene (0.556 mmol) were reacted in 10 mL of dichloromethane for 2 h to give, after slurrying in 3 mL of acetonitrile, vacuum filtration, and washing with 4 × 3 mL of acetonitrile, 0.1805 g of (ClipH$_2$)Pd as orange crystals (96%). ^{1}H NMR (CDCl$_3$): δ 1.18, 1.41 (s, 18H each, ^{t}Bu), 5.73 (s, 2H, N*H*), 6.48 (d, *J* = 2.1 Hz, 2H, H-3), 7.05 (d, *J* = 2.2 Hz, 2H, H-5), 7.30 (d, *J* = 8.1 Hz, 2H, H-6′), 7.36 (dd, *J* = 7.3 and 1.8 Hz, 2H, H-3′), 7.41 (td, *J* = 7.3 and 1.2 Hz, 2H, H-4′), 7.46 (td, *J* = 7.8 and 1.75 Hz, 2H, H-5′). ^{13}C{^{1}H} NMR (CDCl$_3$): δ 29.55, 31.93 (C(*C*H$_3$)$_3$), 34.19, 35.56 (*C*(CH$_3$)$_3$), 118.99, 119.49, 123.69, 126.11, 126.84, 127.35, 130.96, 130.99, 136.84, 140.29, 145.58, 166.96 (CO). IR (cm^{-1}): 3215 (w, ν_{NH}), 2951 (m), 2905 (w), 2866 (w), 1607 (w), 1565 (w), 1472 (m), 1440 (m), 1409 (m), 1360 (m), 1300 (m), 1256 (s), 1202 (w), 1161 (w), 1122 (w), 1001 (w), 962 (w), 917 (w), 871 (m), 830 (s), 766 (s), 691 (m). Anal. Calcd for $C_{40}H_{48}N_2O_2Pd$: C, 69.10; H, 6.96; N, 4.03. Found: C, 68.93; H, 6.82; N, 4.40.

(^{t}BuClipH$_2$)Pt. Into a glass bomb were placed 0.2065 g of (^{t}BuClip)Pt (0.230 mmol), 24.6 mg of 10 wt % palladium on carbon (Aldrich; 0.023 mmol Pd, 10 mol %), and a stirbar. Dry benzene (10 mL) was vacuum transferred into the bomb and the mixture allowed to warm to room temperature under vacuum. The bomb was then backfilled with an atmosphere of hydrogen gas and the solution stirred for 4 h to give a colorless solution. The bomb was taken into the drybox and the reaction mixture filtered through a fritted funnel to remove Pd/C. The eluate was collected in a 25 mL round-bottom flask and the solvent removed in vacuo on the vacuum line. The solid was suspended in 3 mL of acetonitrile, collected via vacuum filtration on a fine-porosity fritted funnel, and washed with 2 × 3 mL of acetonitrile. The product was air-dried for 1 h, yielding 0.1444 g of (^{t}BuClipH$_2$)Pt (70%). ^{1}H NMR (CDCl$_3$): δ 1.20, 1.28, 1.47 (s, 18H each, ^{t}Bu), 6.58 (d, *J* = 2.1 Hz, 2H, H-3), 6.60 (s, 2H, N*H*), 7.04 (d, *J* = 2.2 Hz, 2H, H-5), 7.20 (d, *J* = 1.4 Hz, 2H, H-3′), 7.32 (d, *J* = 7.9 Hz, 2H, H-6′), 7.35 (dd, *J* = 7.9 and 1.7 Hz, 2H, H-5′). ^{13}C{^{1}H} NMR (CDCl$_3$): δ 29.71, 31.30, 31.96 (C(*C*H$_3$)$_3$), 34.13, 35.33, 35.60 (*C*(CH$_3$)$_3$), 115.72, 119.01, 123.48, 123.54, 124.78, 127.61, 131.00, 137.02, 139.55, 146.93, 154.31, 168.40 (CO). IR (cm^{-1}): 3200 (w, ν_{NH}), 2953 (m), 2928 (w), 2900 (w), 2863 (w), 1616 (w), 1602 (w), 1473 (m), 1442 (m), 1409 (m), 1364 (m), 1358 (w), 1352 (w), 1298 (m), 1270 (m), 1259 (m), 1252 (s), 1234 (w), 1202 (w), 1116 (w), 1034 (m), 968 (w), 921 (w), 901 (m), 873 (m), 829 (s), 814 (w), 769 (m), 743 (m), 718 (w), 691 (m). Anal. Calcd for $C_{48}H_{66}N_2O_2Pt$: C, 64.19; H, 7.41; N, 3.12. Found: C, 64.45; H, 7.65; N, 3.00.

EPR Spectroscopy. In the drybox, 9.9 mg of (^{t}BuClipH$_2$)Pd and 10.4 mg of (^{t}BuClip)Pd were mixed in 0.6 mL of toluene-d_8, and the solution was monitored by NMR to assess the degree of equilibration of the comproportionation reaction. After the reaction had reached equilibrium, a 100 μL aliquot of this solution was diluted to 10 mL in toluene, and 1.0 mL of this solution was further diluted to 5.0 mL in toluene. This most dilute solution (~80 μM in total palladium) was analyzed by EPR spectroscopy in a screw-cap-sealed 3 mm quartz tube at ambient temperature in a Bruker EMX X-band (9.624 GHz) EPR spectrometer. Spectra were acquired with a power of 20.02 mW and a modulation amplitude of 1.00 G. Spectra were simulated using the MATLAB toolbox program *EasySpin 5.2.11* (easyspin.org).

Azoarene/Hydrazoarene Equilibration Experiments. Hydrazobenzene, azobenzene, and 4,4′-azobenzenedicarboxylate dimethyl ester were commercially available (TCI) and were used as received. 4-Nitroazobenzene was prepared by the condensation of nitrosobenzene with 4-nitroaniline.[34] Other 4,4′-disubstituted azobenzenes (X = Br, NO$_2$, or CN) were prepared by the oxidative coupling of the corresponding anilines using *tert*-butyl hypoiodite.[35] In order to measure the hydrogen atom transfer equilibrium between two azo compounds, the following procedure was used. To a J. Young NMR tube in the drybox were added approximately 0.007 g of the less oxidizing azo compound, 0.002 g of 10% Pd/C, and 0.6 mL of THF-d_8. The tube was removed from the drybox and the solution frozen in liquid nitrogen. The Teflon seal was unscrewed, and 50 μL of a 5% (v/v) solution of hydrazine hydrate in THF-d_8 was immediately syringed into the NMR tube, after which the tube was resealed. While the solution was still frozen, the NMR tube was attached to a vacuum line and degassed for 5 min. The reaction with hydrazine was monitored via ^{1}H NMR, and if the reaction was incomplete in 1 day, an additional 30 μL of 5% hydrazine hydrate in THF-d_8 was added, which invariably caused the reaction to go to completion after 1 day of further reaction. (When azobenzene was the less oxidizing azo compound, hydrazobenzene was used directly instead of being generated in situ by hydrazine reduction.) Chemical shifts in THF-d^8 of the azo- and hydrazobenzenes studied are given in Table S1.

The NMR tube was then brought into the drybox, where approximately 7 mg of the more oxidizing azo compound was added, and the solution thoroughly mixed. The equilibrium was then measured over the course of several days via integration of the ^{1}H NMR spectra; in all cases, equilibration was achieved within 2 days, as judged by the subsequent constancy of the NMR spectra.

Kinetics of Reactions of Oxygen Radicals with (^{t}BuClipH$_2$)M. In the drybox, a 1 mM (^{t}BuClipH$_2$)M solution was prepared by dissolving 0.01 g of the complex in 10 mL of toluene in a 20 mL glass vial. In reactions with lower concentrations of oxygen radicals, a 10-

fold dilution of the above solution was carried out to maintain pseudo-first-order conditions during the kinetic runs. Stock solutions of the organic radical of the desired concentration were prepared in toluene. In the drybox, 2 mL of the appropriate organic radical stock solution was dispensed into the cuvette compartment of an angled-reservoir Teflon-sealed (ARTS) cuvette (see the Supporting Information for photographs), followed by the addition of 50 μL of the (^{t}BuClipH$_2$)M solution to the reservoir of the cuvette. The cuvette was then sealed with a Teflon plug and brought to the UV−vis instrument. The cell was equilibrated at 23 °C in a cell block whose temperature was maintained using a recirculating bath, and the spectrometer was blanked using a solution of the radical. The reaction was initiated by inverting the ARTS cell, and spectra were obtained while illuminating the sample using only the visible lamp. Absorbances at λ_{max} of the (^{t}BuClip)M complex as a function of time were fit either to first-order kinetics or, in the case of reactions of the palladium complex with nitroxyl radicals, to successive first-order reactions with fixed ε values for (^{t}BuClip)Pd and (^{t}BuClipH)Pd. Pseudo-first-order rate constants varied linearly with the concentration of the oxygen radicals (Figures S1), and second-order rate constants were determined from the slopes of the plots of k_{obs} versus [RO$^\bullet$].

X-ray Crystallography. Crystals of (ClipH$_2$)Pd·C$_4$D$_8$O were deposited after a reaction mixture of (Clip)Pd with PhNHNHPh in THF-d_8 was mixed with hexane and allowed to evaporate slowly in air. Crystals were placed in Paratone oil before being transferred to the cold dinitrogen stream of the diffractometer. Initial attempts to run the experiments at 120 K resulted in crystal fracturing, so data were collected at 200 K. Data were reduced and corrected for absorption using the program *SADABS*. The structure was solved using direct methods, and non-hydrogen atoms not apparent from the initial solutions were found on difference Fourier maps.

Both the *tert*-butyl group centered on C18 and the one centered on C28 were disordered over two orientations. In each case, the disorder was modeled by constraining opposite methyl groups in the two components to have equal thermal parameters and allowing the occupancies to refine; the refined occupancies of the major components were 68.6(6)% and 55.7(6)%, respectively. The THF-d_8 molecule displayed two different orientations for the middle CH$_2$CH$_2$ moiety (C52/C521 and C53/C531), which were modeled analogously. The major orientation refined to 65.5(15)% occupancy.

Deuterium atoms on the solvent and hydrogen atoms on the disordered *tert*-butyl groups were placed in calculated positions with thermal parameters 1.5 times (for CH$_3$) and 1.2 times (for CD$_2$) that of the carbon atoms to which they were attached. All other hydrogen atoms were found on difference maps and refined isotropically. Calculations used *SHELXTL* (Bruker AXS),[36] with scattering factors and anomalous dispersion terms taken from the literature.[37] Further details about the structure are given in Table 1.

Computational Methods. Computationally, the *tert*-butyl groups in (^{t}BuClip)M and (^{t}BuClipH$_2$)M were replaced with hydrogen atoms. Geometry optimizations were performed on all compounds as singlet gas-phase molecules using a B3LYP functional, with an SDD basis set for the palladium or platinum atom and a 6-31G* basis set for all other atoms, using the program *Gaussian09*.[38] Geometries were optimized by minimizing the energies of the compounds, and optimized geometries were confirmed to be minima by the lack of imaginary frequencies in vibrational analysis.

■ ASSOCIATED CONTENT

Ⓢ Supporting Information

The Supporting Information is available free of charge on the ACS Publications website at DOI: 10.1021/acs.inorgchem.8b00068.

> Plots of k_{obs} versus [RO$^\bullet$], descriptions of the ^{1}H NMR spectra of azo- and hydrazobenzenes in THF-d_8, photographs of the ARTS cuvettes, and energies and Cartesian coordinates of DFT-optimized structures (PDF)

Accession Codes

CCDC 1815092 contains the supplementary crystallographic data for this paper. These data can be obtained free of charge via www.ccdc.cam.ac.uk/data_request/cif, or by emailing data_request@ccdc.cam.ac.uk, or by contacting The Cambridge Crystallographic Data Centre, 12 Union Road, Cambridge CB2 1EZ, UK; fax: +44 1223 336033.

■ AUTHOR INFORMATION

Corresponding Author

*E-mail: Seth.N.Brown.114@nd.edu.

ORCID

Seth N. Brown: 0000-0001-8414-2396

Notes

The authors declare no competing financial interest.

■ ACKNOWLEDGMENTS

This work was supported by the U.S. National Science Foundation (Grant CHE-1465104). We gratefully acknowledge the assistance of Dr. Allen G. Oliver with X-ray crystallography.

■ REFERENCES

(1) Mayer, J. M. Hydrogen Atom Abstraction by Metal—Oxo Complexes: Understanding the Analogy with Organic Radical Reactions. *Acc. Chem. Res.* **1998**, *31*, 441−450.

(2) Forrester, A. R.; Hay, J. M.; Thomson, R. H. *Organic Chemistry of Stable Free Radicals*; Academic Press: New York, 1968.

(3) (a) Pierpont, C. G. Studies on charge distribution and valence tautomerism in transition metal complexes of catecholate and semiquinonate ligands. *Coord. Chem. Rev.* **2001**, *216−217*, 99−125. (b) Pierpont, C. G. Unique properties of transition metal quinone complexes of the MQ$_3$ series. *Coord. Chem. Rev.* **2001**, *219−221*, 415−433. (c) Pierpont, C. G. Ligand Redox Activity and Mixed Valency in First-Row Transition-Metal Complexes Containing Tetrachlorocatecholate and Radical Tetrachlorosemiquinonate Ligands. *Inorg. Chem.* **2011**, *50*, 9766−9772.

(4) (a) Lyaskovskyy, V.; de Bruin, B. Redox Non-Innocent Ligands: Versatile New Tools to Control Catalytic Reactions. *ACS Catal.* **2012**, *2*, 270−279. (b) Munhá, R. F.; Zarkesh, R. A.; Heyduk, A. F. Group transfer reactions of d^0 transition metal complexes: redox-active ligands provide a mechanism for expanded reactivity. *Dalton Trans.* **2013**, *42*, 3751−3766. (c) Broere, D. L. J.; Plessius, R.; van der Vlugt, J. I. New avenues for ligand-mediated processes — expanding metal reactivity by the use of redox-active catechol, *o*-aminophenol and *o*-phenylenediamine ligands. *Chem. Soc. Rev.* **2015**, *44*, 6886−6915. (d) Sarkar, B.; Schweinfurth, D.; Deibel, N.; Weisser, F. *Coord. Chem. Rev.* **2015**, *293−294*, 250−262.

(5) Tsang, W. Heats of Formation of Organic Free Radicals by Kinetic Methods. In *Energetics of Organic Free Radicals*; Martinho Simões, J. A., Greenberg, A., Liebman, J. F., Eds.; Blackie Academic and Professional: London, 1996; pp 22−58.

(6) Ogliaro, F.; Harris, N.; Cohen, S.; Filatov, M.; de Visser, S. P.; Shaik, S. A Model "Rebound" Mechanism of Hydroxylation by Cytochrome P450: Stepwise and Effectively Concerted Pathways, and Their Reactivity Patterns. *J. Am. Chem. Soc.* **2000**, *122*, 8977−8989.

(7) Kumar, A.; Bhatti, T. M.; Goldman, A. S. Dehydrogenation of Alkanes and Aliphatic Groups by Pincer-Ligated Metal Complexes. *Chem. Rev.* **2017**, *117*, 12357−12384.

(8) Warren, J. J.; Tronic, T. A.; Mayer, J. M. Thermochemistry of Proton-Coupled Electron Transfer Reagents and its Implications. *Chem. Rev.* **2010**, *110*, 6961−7001.

(9) Chaudhuri, P.; Verani, C. N.; Bill, E.; Bothe, E.; Weyhermüller, T.; Wieghardt, K. Electronic Structure of Bis(*o*-iminobenzosemiquinonato)metal Complexes (Cu, Ni, Pd). The Art of Establishing Physical Oxidation States in Transition-Metal

Complexes Containing Radical Ligands. *J. Am. Chem. Soc.* **2001**, *123*, 2213−2223.

(10) Mukherjee, C.; Weyhermüller, T.; Bothe, E.; Chaudhuri, P. Targeted Oxidase Reactivity with a New Redox-Active Ligand Incorporating N_2O_2 Donor Atoms. Complexes of Cu(II), Ni(II), Pd(II), Fe(III), and V(V). *Inorg. Chem.* **2008**, *47*, 11620−11632.

(11) Sun, X.; Chun, H.; Hildenbrand, K.; Bothe, E.; Weyhermüller, T.; Neese, F.; Wieghardt, K. *o*-Iminobenzosemiquinonato(1−) and *o*-Amidophenolato(2−) Complexes of Palladium(II) and Platinum(II): A Combined Experimental and Density Functional Theoretical Study. *Inorg. Chem.* **2002**, *41*, 4295−4303.

(12) Min, K. S.; Weyhermüller, T.; Bothe, E.; Wieghardt, K. Tetradentate Bis(*o*-iminobenzosemiquinonato(1−)) π Radical Ligands and Their *o*-Aminophenolate(1−) Derivatives in Complexes of Nickel(II), Palladium(II), and Copper(II). *Inorg. Chem.* **2004**, *43*, 2922−2931.

(13) Kokatam, S.; Weyhermüller, T.; Bothe, E.; Chaudhuri, P.; Wieghardt, K. Structural Characterization of Four Members of the Electron-Transfer Series $[\mathrm{Pd}^{\mathrm{II}}(\mathrm{L})_2]^n$ (L = *o*-Iminophenolate Derivative; n = 2−, 1−, 0, 1+, 2+). Ligand Mixed Valency in the Monocation and Monoanion with $S = 1/2$ Ground States. *Inorg. Chem.* **2005**, *44*, 3709−3717.

(14) Swanson, D. D.; Conner, K. M.; Brown, S. N. A chelating bis(aminophenol) ligand bridged by a 1,1′-ferrocene-bis(*para*-phenylene) linker. *Dalton Trans.* **2017**, *46*, 9049−9057.

(15) Herebian, D.; Wieghardt, K. E.; Neese, F. Analysis and Interpretation of Metal-Radical Coupling in a Series of Square Planar Nickel Complexes: Correlated Ab Initio and Density Functional Investigation of $[\mathrm{Ni}(\mathrm{L}^{\mathrm{ISQ}})_2]$ ($\mathrm{L}^{\mathrm{ISQ}}$=3,5-di-*tert*-butyl-*o*-diiminobenzosemiquinonate(1-)). *J. Am. Chem. Soc.* **2003**, *125*, 10997−11005.

(16) Conner, K. M.; Perugini, A. L.; Malabute, M.; Brown, S. N. Group 10 Bis(iminosemiquinone) Complexes: Measurement of Singlet-Triplet Gaps and Analysis of the Effects of Metal and Geometry on Electronic Structure. *Inorg. Chem.* **2018**, DOI: 10.1021/acs.inorgchem.8b00062.

(17) Deibel, N.; Hohloch, S.; Schweinfurth, D.; Weisser, F.; Grupp, A.; Sarkar, B. Three-Way Cooperativity in d^8 Metal Complexes with Ligands Displaying Chemical and Redox Non-Innocence. *Chem. - Eur. J.* **2014**, *20*, 15178−15187.

(18) Kopec, J. A.; Shekar, S.; Brown, S. N. Molybdenum(VI) Complexes of a 2,2′-Biphenyl-bridged Bis(amidophenoxide): Competition between Metal−Ligand and Metal−Amidophenoxide π Bonding. *Inorg. Chem.* **2012**, *51*, 1239−1250.

(19) Broere, D. L. J.; Demeshko, S.; de Bruin, B.; Pidko, E. A.; Reek, J. N. H.; Siegler, M. A.; Lutz, M.; van der Vlugt, J. I. Dinuclear Palladium Complexes with Two Ligand-Centered Radicals and a Single Bridging Ligand: Subtle Tuning of Magnetic Properties. *Chem. - Eur. J.* **2015**, *21*, 5879−5886.

(20) Broere, D. L. J.; Metz, L. L.; de Bruin, B.; Reek, J. N. H.; Siegler, M. A.; van der Vlugt, J. I. Redox-Active Ligand-Induced Homolytic Bond Activation. *Angew. Chem., Int. Ed.* **2015**, *54*, 1516−1520.

(21) Broere, D. L. J.; van Leest, N. P.; de Bruin, B.; Siegler, M. A.; van der Vlugt, J. I. Reversible Redox Chemistry and Catalytic $\mathrm{C(sp^3)}$−H Amination Reactivity of a Paramagnetic Pd Complex Bearing a Redox-Active *o*-Aminophenol-Derived NNO Pincer Ligand. *Inorg. Chem.* **2016**, *55*, 8603−8611.

(22) Broere, D. L. J.; de Bruin, B.; Reek, J. N. H.; Lutz, M.; Dechert, S.; van der Vlugt, J. I. Intramolecular Redox-Active Ligand-to-Substrate Single-Electron Transfer: Radical Reactivity with a Palladium(II) Complex. *J. Am. Chem. Soc.* **2014**, *136*, 11574−11577.

(23) (a) Deibel, N.; Schweinfurth, D.; Hohloch, S.; Fiedler, J.; Sarkar, B. Donor−acceptor systems of Pt(II) and redox-induced reactivity towards small molecules. *Chem. Commun.* **2012**, *48*, 2388−2390. (b) Deibel, N.; Schweinfurth, D.; Hohloch, S.; Delor, M.; Sazanovich, I. V.; Towrie, M.; Weinstein, J. A.; Sarkar, B. Electrochemistry, Chemical Reactivity, and Time-Resolved Infrared Spectroscopy of Donor−Acceptor Systems $[(\mathrm{Q}^x)\mathrm{Pt}(\mathrm{pap}^y)]$ (Q = Substituted *o*-Quinone or *o*-Iminoquinone; pap = Phenylazopyridine). *Inorg. Chem.* **2014**, *53*, 1021−1031.

(24) Mahoney, L. R.; Ferris, F. C.; DaRooge, M. A. Calorimetric Study of the 2,4,6-Tri-*t*-butylphenoxy Radical in Solution. *J. Am. Chem. Soc.* **1969**, *91*, 3883−3889.

(25) Mader, E. A.; Manner, V. W.; Markle, T. F.; Wu, A.; Franz, J. A.; Mayer, J. M. Trends in Ground-State Entropies for Transition Metal Based Hydrogen Atom Transfer Reactions. *J. Am. Chem. Soc.* **2009**, *131*, 4335−4345.

(26) Jackson, W. G.; Harrowfield, J. M.; Vowles, P. D. Consecutive, Irreversible First-Order Reactions. Ambiguities and Practical Aspects of Kinetic Analysis. *Int. J. Chem. Kinet.* **1977**, *9*, 535−548.

(27) Lucarini, M.; Pedulli, G. F.; Cipollone, M. Bond Dissociation Enthalpy of α-Tocopherol and Other Phenolic Antioxidants. *J. Org. Chem.* **1994**, *59*, 5063−5070.

(28) Goldstein, S.; Russo, A.; Samuni, A. Reactions of PTIO and Carboxy-PTIO with •NO, $\bullet\mathrm{NO_2}$, and $\mathrm{O_2}\bullet^-$. *J. Biol. Chem.* **2003**, *278*, 50949−50955.

(29) Billone, P. S.; Johnson, P. A.; Lin, S.; Scaiano, J. C.; DiLabio, G. A.; Ingold, K. U. Accurate O−H Bond Dissociation Energy Differences of Hydroxylamines Determined by EPR Spectroscopy: Computational Insight into Stereoelectronic Effects on BDEs and EPR Spectral Parameters. *J. Org. Chem.* **2011**, *76*, 631−636.

(30) Mahoney, L. R.; Mendenhall, G. D.; Ingold, K. U. Calorimetric and Equilibrium Studies on Some Stable Nitroxide and Iminoxy Radicals. Approximate O−H Bond Dissociation Energies in Hydroxylamines and Oximes. *J. Am. Chem. Soc.* **1973**, *95*, 8610−8614.

(31) Sen, V. D.; Tikhonov, I. V.; Borodin, L. I.; Pliss, E. M.; Golubev, V. A.; Syroeshkin, M. A.; Rusakov, A. I. Kinetics and thermodynamics of reversible disproportionation−comproportionation in redox triad oxoammonium cations − nitroxyl radicals − hydroxylamines. *J. Phys. Org. Chem.* **2015**, *28*, 17−24.

(32) Carter, S. M.; Sia, A.; Shaw, M. J.; Heyduk, A. F. Isolation and Characterization of a Neutral Imino-semiquinone Radical. *J. Am. Chem. Soc.* **2008**, *130*, 5838−5839.

(33) Evans, M. G.; Polanyi, M. Inertia and Driving Force of Chemical Reactions. *Trans. Faraday Soc.* **1938**, *34*, 11−24.

(34) Slavov, C.; Yang, C.; Schweighauser, L.; Boumrifak, C.; Dreuw, A.; Wegner, H. A.; Wachtveitl, J. Connectivity matters — ultrafast isomerization dynamics of bisazobenzene photoswitches. *Phys. Chem. Chem. Phys.* **2016**, *18*, 14795−14804.

(35) Okumura, S.; Lin, C.-H.; Takeda, Y.; Minakata, S. Oxidative Dimerization of (Hetero)aromatic Amines Utilizing *t*-BuOI Leading to (Hetero)aromatic Azo Compounds: Scope and Mechanistic Studies. *J. Org. Chem.* **2013**, *78*, 12090−12105.

(36) Sheldrick, G. M. A short history of *SHELX*. *Acta Crystallogr., Sect. A: Found. Crystallogr.* **2008**, *64*, 112−122.

(37) *International Tables for Crystallography*; Kluwer Academic Publishers: Dordrecht, The Netherlands, 1992; Vol C.

(38) Frisch, M. J.; Trucks, G. W.; Schlegel, H. B.; Scuseria, G. E.; Robb, M. A.; Cheeseman, J. R.; Scalmani, G.; Barone, V.; Mennucci, B.; Petersson, G. A.; Nakatsuji, H.; Caricato, M.; Li, X.; Hratchian, H. P.; Izmaylov, A. F.; Bloino, J.; Zheng, G.; Sonnenberg, J. L.; Hada, M.; Ehara, M.; Toyota, K.; Fukuda, R.; Hasegawa, J.; Ishida, M.; Nakajima, T.; Honda, Y.; Kitao, O.; Nakai, H.; Vreven, T.; Montgomery, J. A., Jr.; Peralta, J. E.; Ogliaro, F.; Bearpark, M.; Heyd, J. J.; Brothers, E.; Kudin, K. N.; Staroverov, V. N.; Kobayashi, R.; Normand, J.; Raghavachari, K.; Rendell, A.; Burant, J. C.; Iyengar, S. S.; Tomasi, J.; Cossi, M.; Rega, N.; Millam, J. M.; Klene, M.; Knox, J. E.; Cross, J. B.; Bakken, V.; Adamo, C.; Jaramillo, J.; Gomperts, R.; Stratmann, R. E.; Yazyev, O.; Austin, A. J.; Cammi, R.; Pomelli, C.; Ochterski, J. W.; Martin, R. L.; Morokuma, K.; Zakrzewski, V. G.; Voth, G. A.; Salvador, P.; Dannenberg, J. J.; Dapprich, S.; Daniels, A. D.; Farkas, O.; Foresman, J. B.; Ortiz, J. V.; Cioslowski, J.; Fox, D. J. *Gaussian09*, revision A.02; Gaussian, Inc.: Wallingford, CT, 2009.